Supporting Information for:

Quantifying Biomolecular Interactions using Slow Mixing Mode (SLOMO) Nanoflow ESI-MS

Duong T. Bui,[1] Zhixiong Li,[1] Pavel I. Kitov,[1] Ling Han,[1] Elena N. Kitova,[1] Marlène Fortier,[2] Camille Fuselier,[2] Philippine Granger Joly de Boissel,[2] David Chatenet,[2] Nicolas Doucet,[2] Stephen M. Tompkins,[3,4] Yves St-Pierre,[2] Lara K. Mahal,[1] and John S. Klassen[1]*

[1] *Department of Chemistry, University of Alberta, Edmonton, Alberta, Canada T6G 2G2*

[2] *Centre Armand-Frappier Santé Biotechnologie, Institut National de la Recherche Scientifique (INRS), Université du Québec, Laval, QC, Canada H7V 1B7*

[3] *Center for Vaccines and Immunology, University of Georgia, Athens, GA, USA*

[4] *Emory-UGA Centers of Excellence for Influenza Research and Surveillance (CEIRS), Athens, GA, USA*

* Corresponding Author:

Department of Chemistry

University of Alberta

Edmonton, AB CANADA T6G 2G2

Email: john.klassen@ualberta.ca

Telephone: (780) 492-3501

Fax: (780) 492-8231

Table of Contents

Materials and Methods

Production of recombinant human galectins and nanobody.

Recombinant human galectins were purified as previously described[S1] using pET-22b(+) vectors encoding the respective cDNA for human galectin-1,-3, -7 and -13. The recombinant proteins were produced in *E.coli* BL21 (DE3) cells and purified by affinity chromatography using lactose (or mannose in the case of GAL-13) using standard protocols.[S2] Production and purification of the GAL-7-specific nanobody (sdAB) was also carried out in *E. coli* cells using the basic pHEN2 vector followed by standard metal (Ni)-affinity chromatography (His GraviTrap, Sigma-Aldrich, Oakville, Canada).

Quantification of binding affinity of sdAb-GAL-7 complex to LNT

Quantification of sdAB-GAL-7 binding in the presence of LNT and GAL-7 binding to LNT was performed simultaneously using SLOMO. 2-3 μL of ammonium acetate (200 mM, pH 7.4) solution of sdAb (3 μM), GAL-7 (2-6 μM) and LNT (50 μM) was loaded followed by 10 μL of solution of sdAb (3 μM), GAL-7 (40 μM) and LNT (50 μM). In the sdAb-GAL-7-LNT mixture, LNT binds to GAL-7 monomer, GAL-7 dimer and sdAb-GAL-7 complex. When GAL-7 monomer and dimer are treated as one species and the binding sites are counted (P_1), there are two type of complexes with LNT: GAL-7-LNT (P_1L) and sdAb-GAL-7-LNT (P_1P_2L). The following equilibria exist in the solution (eqs S1-3):

$$P_1L \rightleftharpoons P_1 + L \quad \text{(S1)}$$

$$P_1P_2 \rightleftharpoons P_1 + P_2 \quad \text{(S2)}$$

$$P_1P_2L \rightleftharpoons P_1P_2 + L \quad \text{(S3)}$$

The dissociation constant (K_d) for each equilibrium can be calculated using eqs S4-6:

$$K_{d,1} = \frac{[P_1][L]}{[P_1L]} \quad \text{(S4)}$$

$$K_{d,2} = \frac{[P_1][P_2]}{[P_1P_2]} \quad \text{(S5)}$$

$$K_{d,3} = \frac{[P_1P_2][L]}{[P_1P_2L]} \quad \text{(S6)}$$

The mass balance for the species in the solution can be expressed by eqs S7-9:

$$[L]_0 = [L] + [P_1L] + [P_1P_2L] \quad \text{(S7)}$$

$$[P_1]_0 = [P_1] + [P_1L] + [P_1P_2] + [P_1P_2L] \quad \text{(S8)}$$

$$[P_2]_0 = [P_2] + [P_1P_2] + [P_1P_2L] \quad \text{(S9)}$$

From eq S9, each concentration can be expressed in term of sum of corresponding ion abundances (*Ab*), eqs S10-12:

$$[P_2] = \frac{Ab(P_2)[P_2]_0}{Ab(P_2) + RF_{P_2/P_1P_2} Ab(P_1P_2) + RF_{P_2/P_1P_2} Ab(P_1P_2L)} \quad \text{(S10)}$$

$$[P_1P_2] = \frac{RF_{P_2/P_1P_2} Ab(P_1P_2)[P_2]_0}{Ab(P_2) + RF_{P_2/P_1P_2} Ab(P_1P_2) + RF_{P_2/P_1P_2} Ab(P_1P_2L)} \quad \text{(S11)}$$

$$[P_1P_2L] = \frac{RF_{P_2/P_1P_2} Ab(P_1P_2L)[P_2]_0}{Ab(P_2) + RF_{P_2/P_1P_2} Ab(P_1P_2) + RF_{P_2/P_1P_2} Ab(P_1P_2L)} \quad \text{(S12)}$$

where RF_{P_2/P_1P_2} is the relative response factor of sdAb (P_2) over sdAb-GAL-7 (P_1P_2) calculated using SLOMO. The value of $[P_1]$ is then calcualted using eq S13:

$$[P_1] = \frac{K_{d,2}[P_1P_2]}{[P_2]} \quad \text{(S13)}$$

and $[P_1L]$ calculated using eq S14:

$$[\mathrm{P_1L}] = [\mathrm{P_1}]_0 - \frac{K_{\mathrm{d},2}[\mathrm{P_1P_2}]}{[\mathrm{P_2}]} - [\mathrm{P_1P_2}] - [\mathrm{P_1P_2L}] \quad \text{(S14)}$$

and [L] using eqs S15a-b:

$$[\mathrm{L}] = [\mathrm{L}]_0 - [\mathrm{P_1L}] - [\mathrm{P_1P_2L}] = [\mathrm{L}]_0 - [\mathrm{P_1}]_0 + \frac{K_{\mathrm{d},2}[\mathrm{P_1P_2}]}{[\mathrm{P_2}]} + [\mathrm{P_1P_2}] \quad \text{(S15a)}$$

$$[\mathrm{L}] = [\mathrm{L}]_0 - [\mathrm{P_1}]_0 + \frac{K_{\mathrm{d},2} RF_{\mathrm{P_2/P_1P_2}} Ab(\mathrm{P_1P_2})}{Ab(\mathrm{P_2})} + \frac{RF_{\mathrm{P_2/P_1P_2}} Ab(\mathrm{P_1P_2})[\mathrm{P_2}]_0}{Ab(\mathrm{P_2}) + RF_{\mathrm{P_2/P_1P_2}} Ab(\mathrm{P_1P_2}) + RF_{\mathrm{P_2/P_1P_2}} Ab(\mathrm{P_1P_2L})} \quad \text{(S15b)}$$

$K_{\mathrm{d},3}$ is then obtained using eqs S16a-b:

$$K_{\mathrm{d},3} = \frac{Ab(\mathrm{P_1P_2})[\mathrm{L}]}{Ab(\mathrm{P_1P_2L})} \quad \text{(S16a)}$$

$$K_{\mathrm{d},3} = \frac{Ab(\mathrm{P_1P_2})}{Ab(\mathrm{P_1P_2L})}([\mathrm{L}]_0 - [\mathrm{P_1}]_0 + \frac{K_{\mathrm{d},2} RF_{\mathrm{P_2/P_1P_2}} (Ab(\mathrm{P_1P_2})}{Ab(\mathrm{P_2})} + \frac{RF_{\mathrm{P_2/P_1P_2}} Ab(\mathrm{P_1P_2})[\mathrm{P_2}]_0}{Ab(\mathrm{P_2}) + RF_{\mathrm{P_2/P_1P_2}} Ab(\mathrm{P_1P_2}) + RF_{\mathrm{P_2/P_1P_2}} Ab(\mathrm{P_1P_2L})}) \quad \text{(S16b)}$$

Solution mixing in nanoESI tip

To establish the relative contribution of diffusion and electroosmotic and electrophoretic flow to analyte mixing, we performed a series of control experiments. First, we measured the solution flow rate achieved with the nanoESI tips by measuring the distance traveled by the meniscus of the solution in the tip. According to these measurements, the average solution flow rate is 14 ± 4 nL min^{-1}, which is consistent with flow rates reported previously for comparable nanoESI tips. Solvent losses resulting from evaporation were taken into account. Based on the average flow rate and assuming there is no mixing of the solutions, it will take approximately 3.5 h for the *Solution 1* volume to be consumed, which is significantly longer than the times required to observe changes in R_{app}. Next, we assessed the influence of electroosmotic and electrophoretic flow on mixing of the analyte. A series of nanoESI tips were loaded with 3 µL of a solution of Van (2 µM) and AcAA (10 µM), followed by injection of 10 µL of a solution of Van (2 µM) and AcAA (500 µM). The

solutions were incubated on the bench for varying times before performing time-resolved ESI-MS analysis. Notably, the time required to observe significant changes in R_{app} is similar to those measured by continuous ESI-MS analysis (Figure S2). Together, these results suggest that analyte mixing inside the nanoESI tips is dominated by diffusion.

Isothermal titration calorimetry (ITC)

The ITC measurements (of the Van-AcAA complex affinity) were carried out using a Microcal PEAQ ITC (Malvern Panalytical, Worcestershire, United Kingdom). For each experiment, a Van solution (100 μM) in the sample cell was titrated with a solution of AcAA (1.0 mM); both the Van and AcAA were in aqueous ammonium acetate solutions (200 mM, pH 6.9, 25 °C). The experimental parameters used are: 0.4 μL for the first injection, 2 μL/injection for 2-19 injections, reference power 5 μW, duration 0.8 s for the first injection, 4.0 s for the rest, injection interval (spacing) 150 s.

Tables

Table S1. Affinities (K_d) and other parameters (incubation time required to observe solution mixing, R_{app}, $RF_{Van/VanAcAA}$, R and $K_{d,app}$) calculated from SLOMO performed on ammonium acetate (200 mM, pH 6.9, 25 ºC) solutions of Van (2 μM) and AcAA (5 μM – 40 μM).

$[AcAA]_0$ (μM)	Incubation time (min)	R_{app}	$RF_{Van/VanAcAA}$	R	$K_{d,app}$ (μM)	K_d (μM)
5	21	$1.4x10^{-2}$	11.1	0.15	355.2	31.6
5	22	$1.1x10^{-2}$	11.8	0.14	452.6	34.0
5	40	$1.1x10^{-2}$	10.7	0.12	452.6	39.9
10	11	$2.5x10^{-2}$	8.3	0.21	398.0	46.0
10	15	$5.5x10^{-2}$	6.5	0.36	179.9	26.3
10	5	$5.5x10^{-2}$	4.2	0.23	179.9	41.9
20	20	$5.3x10^{-2}$	13.8	0.72	375.5	26.6
20	35	$7.0x10^{-2}$	9.5	0.66	283.9	29.1
20	20	$8.6x10^{-2}$	7.8	0.67	230.7	28.7
30	18	$7.1x10^{-2}$	13.9	0.99	420.7	29.3
30	35	$6.4x10^{-2}$	14.6	0.94	466.9	30.9
30	35	0.11	6.7	0.76	270.9	38.3
40	30	$8.5x10^{-2}$	15.2	1.3	468.7	29.9
40	35	0.12	8.8	1.1	331.6	35.4
40	30	0.11	9.6	1.1	361.8	35.4

Table S2. Summary of the molecular weights (MWs) of the glycoforms (P_i) of RBD and RBD+GAL-3C complex measured by ESI-MS performed in positive ion mode on ammonium acetate solutions (200 mM, pH 7.4) of RBD (5 μM) and GAL-3C (5 μM). The average MWs of free RBD glycoforms were calculated from the m/z values of three charge states; the MWs of the (RBD+GAL-3C) complexes were calculated from m/z measured at two charge states.

P_i	Detected mass-to-charge ratio (*m/z*)			Free RBD MW (Da)[a]	RBD-GAL-3C Complex MW (Da)	RBD-GAL-3C Complex Theoretical MW (Da)
	z = 11	z = 10	z = 9			
P1	2821.1	3103.3	3448.2	31023 ± 2	ND	47349
P2	2829.0	3111.8	3457.6	31108 ± 1	ND	47435
P3	2835.8	3119.3	3465.8	31183 ± 1	47508	47510
P4	2838.4	3122.3	3469.3	31213 ± 2	47540	47540
P5	2842.2	3126.4	3473.4	31253 ± 1	47578	47580
P6	2845.5	3130.0	3477.8	31290 ± 1	ND	47617
P7	2851.9	3137.1	3485.2	31360 ± 2	47683	47686
P8	2855.5	3141.1	3490.3	31401 ± 2	47730	47728
P9	2858.7	3144.5	3494.1	31435 ± 2	47759	47763
P10	2862.2	3148.3	3498.3	31474 ± 1	47800	47801
P11	2865.1	3151.6	3500.9	31503 ± 4	47829	47830
P12	2868.8	3155.6	3505.8	31545 ± 1	47870	47871
P13	2871.8	3158.9	3510.0	31580 ± 1	47906	47906
P14	2875.4	3162.9	3514.4	31619 ± 1	47943	47946
P15	2877.2	3164.9	3516.6	31639 ± 1	ND	47966
P16	2882.1	3170.3	3521.7	31691 ± 4	48018	48017
P17	2885.0	3173.5	3526.3	31726 ± 2	48050	48052
P18	2888.6	3177.4	3530.3	31764 ± 1	48092	48091
P19	2890.5	3179.4	3532.4	31784 ± 1	ND	48110
P20	2891.7	3180.9	3534.3	31799 ± 1	ND	48125
P21	2894.4	3183.9	3537.5	31828 ± 1	48157	48155
P22	2898.3	3188.0	3542.2	31870 ± 1	48196	48197
P23	2901.9	3192.0	3546.6	31910 ± 1	ND	48237
P24	2903.6	3193.9	3548.6	31929 ± 1	ND	48256
P25	2905.1	3195.6	3550.6	31946 ± 1	ND	48272

P26	2908.6	3199.4	3555.1	31985 ± 2	48310	48311
P27	2911.6	3202.7	3558.4	32017 ± 1	48342	48343
P28	2915.3	3206.6	3563.1	32057 ± 1	ND	48384
P29	2918.4	3210.1	3566.8	32091 ± 1	ND	48418
P30	2924.8	3217.2	3574.3	32161 ± 1	48487	48488
P31	2928.3	3221.2	3578.6	32200 ± 2	ND	48527
P32	2931.5	3224.6	3582.7	32236 ± 1	48558	48562
P33	2935.0	3228.5	3587.0	32274 ± 1	ND	48601
P34	2936.8	3230.5	3589.4	32295 ± 1	ND	48622
P35	2938.3	3232.0	3591.0	32310 ± 1	ND	48637
P36	2941.9	3236.0	3595.2	32349 ± 2	ND	48676
P37	2944.8	3239.2	3599.1	32382 ± 1	48706	48709
P38	2948.1	3243.0	3602.9	32418 ± 1	ND	48745
P39	2950.1	3245.1	3605.4	32440 ± 1	ND	48767
P40	2951.3	3246.5	3607.1	32454 ± 1	48778	48781
P41	2955.1	3250.4	3611.4	32494 ± 1	ND	48821
P42	2958.0	3253.7	3615.1	32527 ± 1	48854	48854
P43	2961.4	3257.5	3619.0	32564 ± 1	ND	48891
P44	2963.3	3259.6	3621.6	32586 ± 1	ND	48913
P45	2964.7	3261.2	3623.0	32600 ± 2	48922	48927
P46	2971.3	3268.3	3631.2	32673 ± 1	48995	48999
P47	2978.0	3275.6	3639.1	32745 ± 2	49067	49072
P48	2981.7	3279.5	3644.2	32787 ± 2	ND	49114
P49	2984.3	3282.8	3647.0	32816 ± 2	49146	49143
P50	2987.7	3286.3	3651.3	32853 ± 1	ND	49180
P51	2991.2	3290.3	3655.5	32892 ± 1	49216	49218
P52	2994.8	3294.2	3660.1	32932 ± 1	49253	49258
P53	2996.5	3296.2	3662.3	32951 ± 1	ND	49278
P54	3004.4	3304.8	3671.8	33037 ± 1	49362	49364
P55	3007.6	3308.6	3675.9	33074 ± 2	ND	49401
P56	3017.6	3319.4	3688.0	33183 ± 1	49511	49510
P57	3021.1	3323.0	3692.1	33221 ± 1	ND	49547
P58	3023.0	3325.2	3694.5	33242 ± 1	ND	49569
P59	3024.4	3326.7	3696.3	33257 ± 1	49579	49584
P60	3031.1	3333.9	3703.9	33328 ± 2	49650	49655
P61	3037.6	3341.0	3712.1	33401 ± 1	ND	49728
P62	3044.0	3348.4	3720.4	33474 ± 1	49802	49800

P63	3049.5	3354.4	3726.8	33533 ± 1	ND	49860
P64	3051.3	3356.0	3728.4	33550 ± 3	ND	49877
P65	3056.3	3361.9	3735.3	33609 ± 1	49937	49935
P66	3064.1	3370.4	3744.8	33694 ± 1	50020	50021
P67	3074.4	3381.7	3756.8	33805 ± 3	ND	50132
P68	3082.7	3390.9	3767.6	33899 ± 1	ND	50226

[a.] Errors correspond to one standard deviation.

Figures

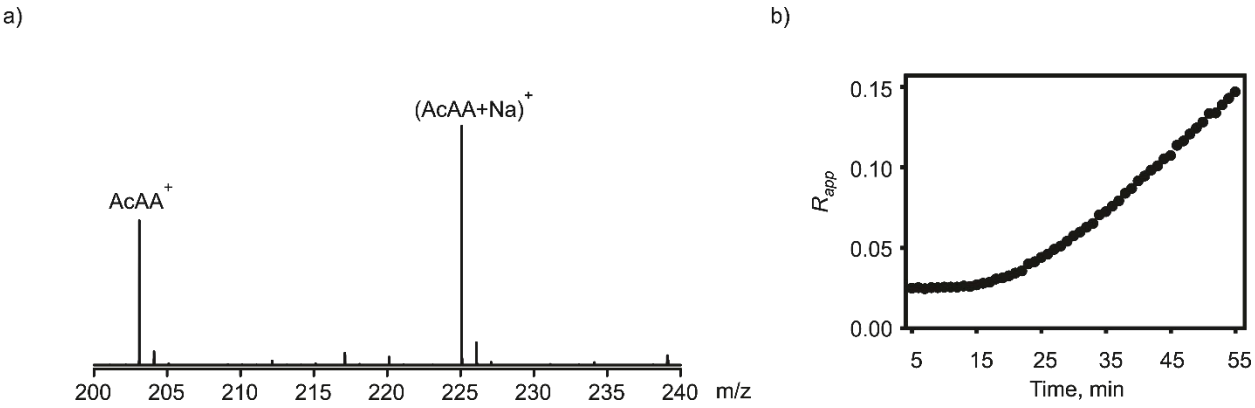

Figure S1. (a) Representative ESI mass spectrum acquired in positive ion mode for a 200 mM ammonium acetate solution (pH 6.9, 25 ºC) of AcAA (20 µM). (b) Time-dependent abundance ratios of the bound (to AcAA) to free Van (R_{app}) measured by SLOMO using 3 µL of *Solution 1* (Van-AcAAVan (2 µM) and AcAA (10 µM)) and 7 µL of *Solution 2* (Van (2 µM) and AcAA (500 µM)).

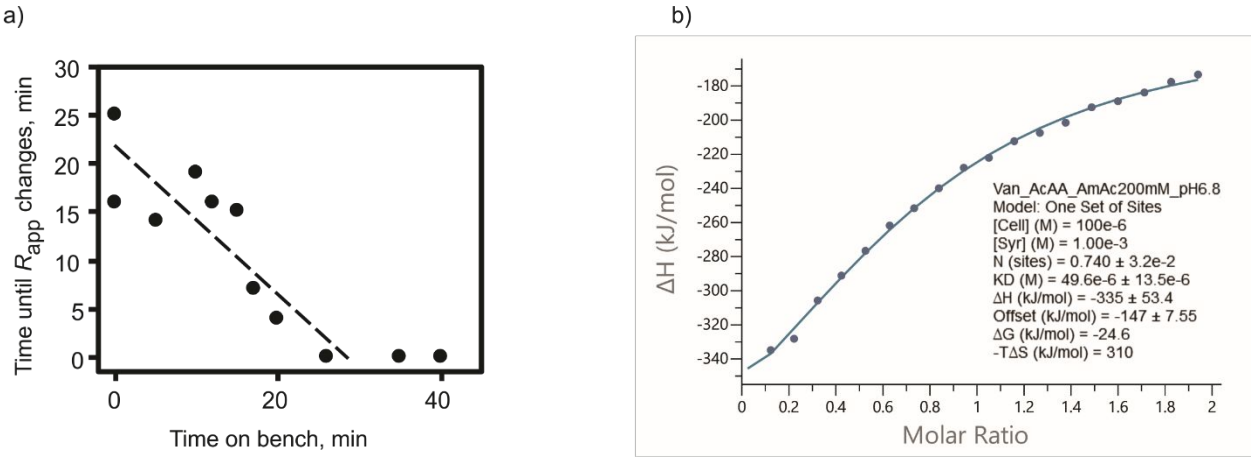

Figure S2. (a) Plot of time required to observe changes in R_{app} measured by SLOMO versus incubation time on bench. Measurements performed using 3 µL of *Solution 1* (Van-AcAAVan (2 µM) and AcAA (10 µM)) and 7 µL of *Solution 2* (Van (2 µM) and AcAA (500 µM)); both solutions were 200 mM ammonium acetate (pH 6.9, 25 ºC). (b) ITC data measured for the binding of Van (100 µM) and AcAA (1 mM) in aqueous ammonium acetate (200 mM, pH 6.9, 25 ºC).

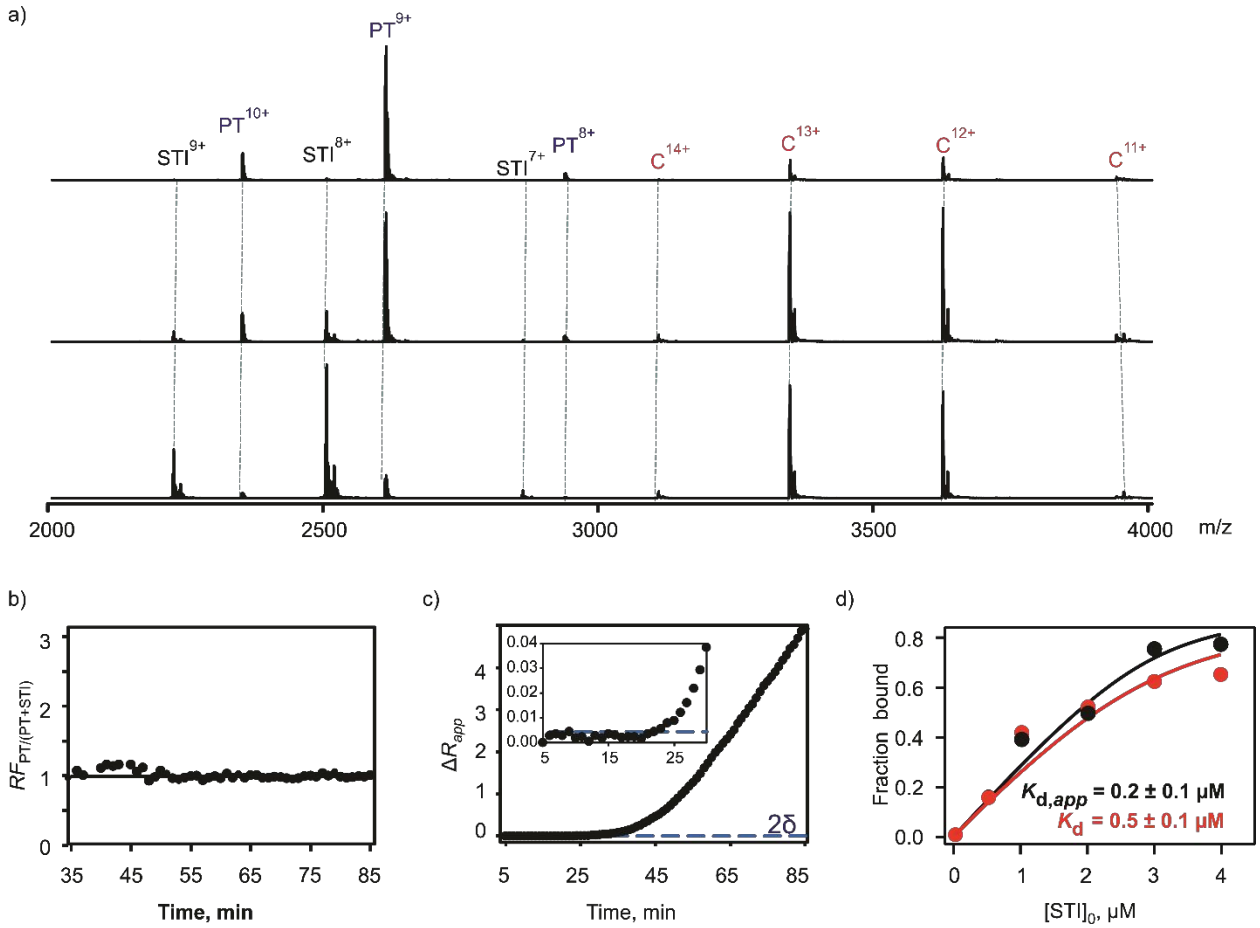

Figure S3. (a) Representative ESI mass spectra acquired in positive ion mode for an ammonium acetate solution (200 mM, pH 4.5) of PT (3 μM) and STI (0.5 μM) at different mixing times. (b) Plot of time-dependent ΔR_{app}. Inset shows ΔR_{app}. values measured at early mixing times (c) Plot of time-dependent relative response factors ($RF_{PT/(PT+STI)}$) measured for PT and the (PT+STI) complex (d) Fraction of bound PT plotted as a function of initial STI concentration determined without (black circles) and with (red circles) consideration of $RF_{PT/C}$. Solid curves represent best fit of eq 11 to the experimental data.

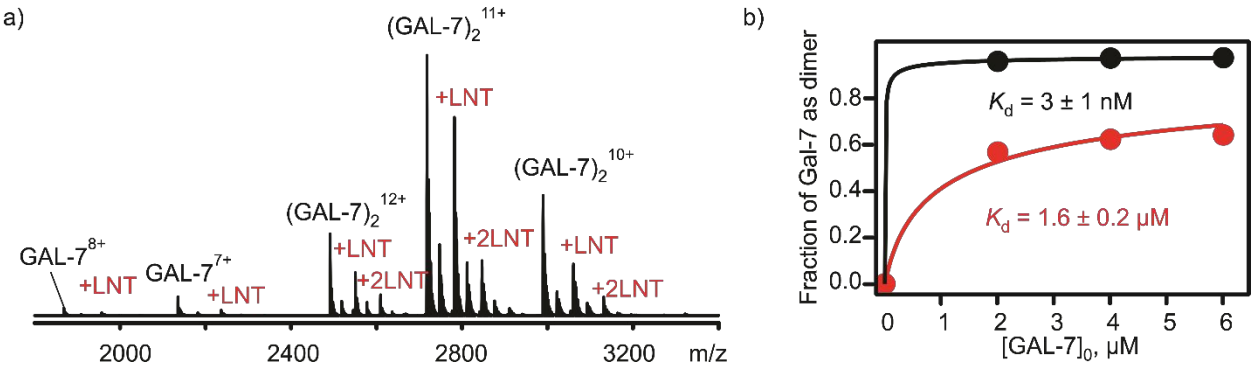

Figure S4. (a) Representative ESI mass spectrum acquired in positive ion mode for a 200 mM ammonium acetate solution (pH 7.4, 25 °C) of GAL-7 (4 μM. (b) Fraction of GAL-7 present as dimer plotted as a function of initial monomer concentration ([GAL-7]$_0$) determined without (black circles) and with (red circles) consideration of $RF_{\text{GAL-7/(GAL-7)}_2}$. Solid curves represent best fit of eq 11 to the experimental data.

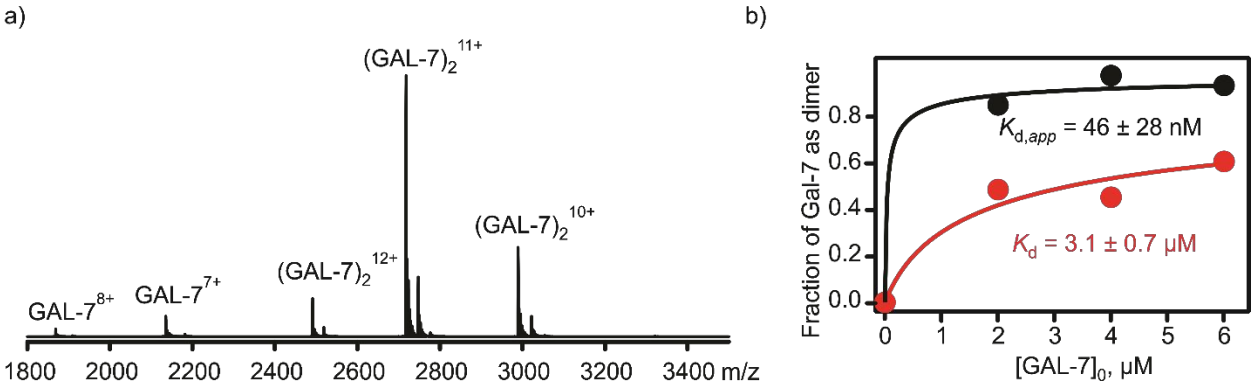

Figure S5. (a) Representative ESI mass spectra acquired in positive ion mode for a 200 mM ammonium acetate solution (pH 7.4, 25 °C) of GAL-7 (2 μM) and LNT (50 μM). (b) Fraction of GAL-7 present as dimer plotted as a function of initial monomer concentration ([GAL-7]$_0$) in the presence of LNT (50 μM) determined without (black circles) and with (red circles) consideration of $RF_{\text{GAL-7/(GAL-7)}_2}$. Solid curves represent best fit of eq 11 to the experimental data acquired in positive ion mode for 200 mM ammonium acetate solution (pH 7.4, 25 °C).

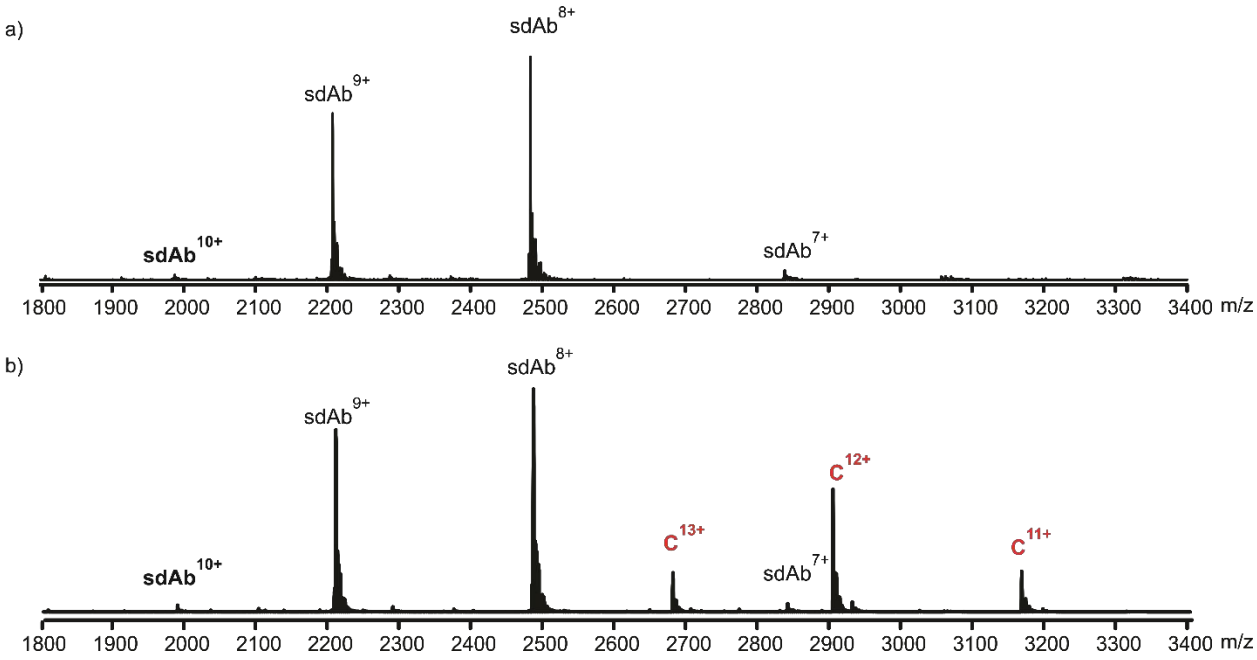

Figure S6. Representative ESI mass spectra acquired in positive ion mode for a 200 mM ammonium acetate solution (pH 7.4, 25 °C) of (a) sdAb (3 μM) and (b) sdAb (3 μM) and GAL-7 (4 μM). The (sdAb+GAL-7) complex is denoted at C.

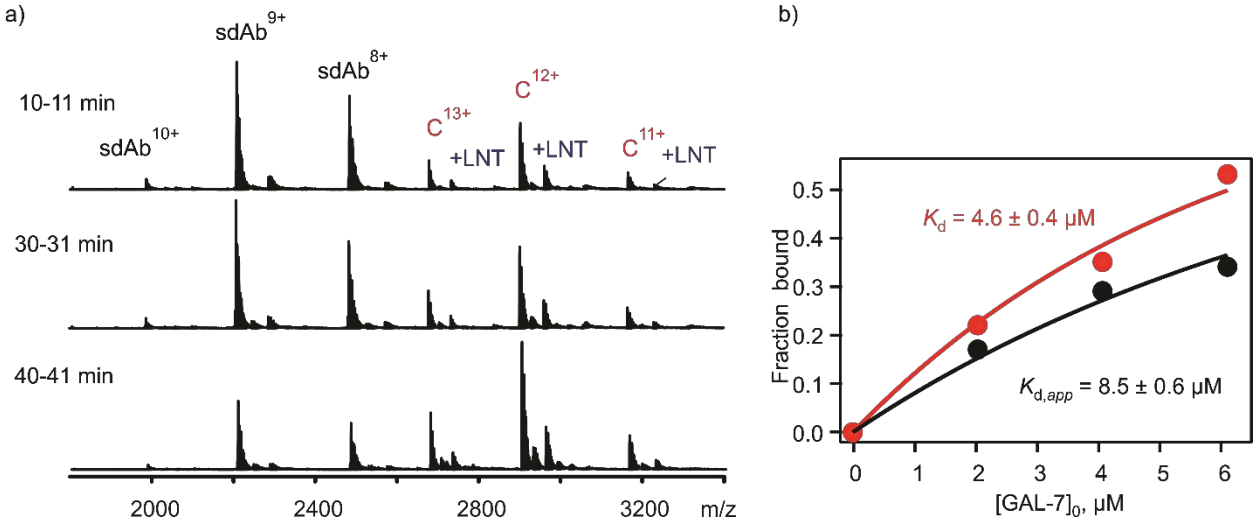

Figure S7. (a) Representative time-resolved ESI mass spectra acquired in positive ion mode for a 200 mM ammonium acetate solution (pH 7.4, 25 °C) of GAL-7 (4 μM), sdAb (4 μM) and LNT (50 μM) (*Solution 1*) and GAL-7 (40 μM), sdAb (4 μM) and L (50 μM) (*Solution 2*). (b) Fraction of bound of sdAb plotted as a function of initial GAL-7 concentration ($[GAL\text{-}7]_0$) determined without (black circles) and with (red circles) consideration of $RF_{sdAb/(sdAb+GAL\text{-}7)}$. Solid curves represent best fit of eq 11 to the experimental data.

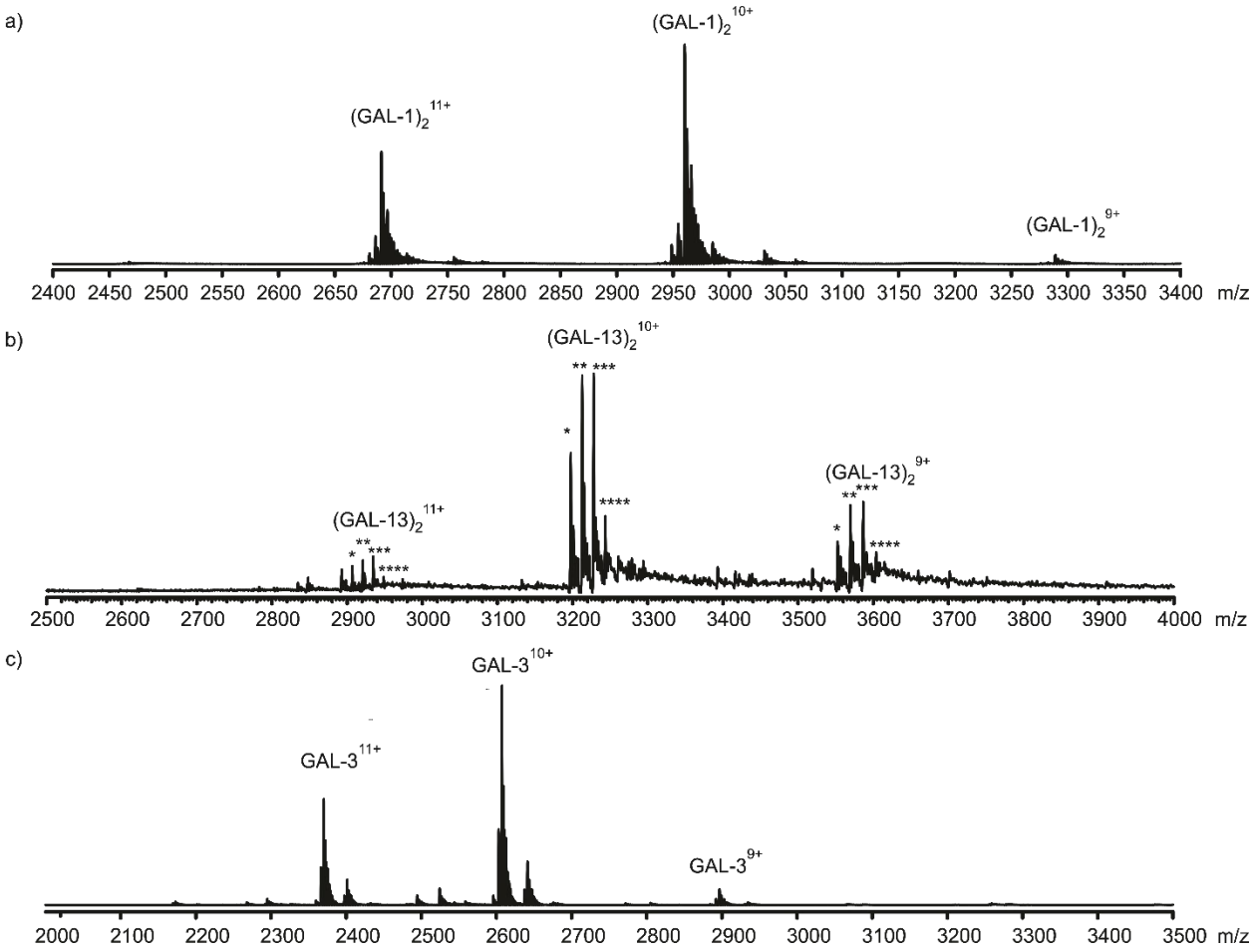

Figure S8. Representative ESI mass spectra acquired in positive ion mode for 200 mM ammonium acetate solutions (pH 7.4, 25 ºC) of (a) GAL-1 (5 µM), (b) GAL-13 (5 µM) and (c) GAL-3 (3 µM). 4 different peaks were detected for GAL-13 because of terminal methionine (M) lost. * GAL-13 dimer minus 2 methionine, ** GAL-13 dimer minus methionine, *** GAL-13 dimer, **** unidentified post-translation modification of GAL-13 dimer.

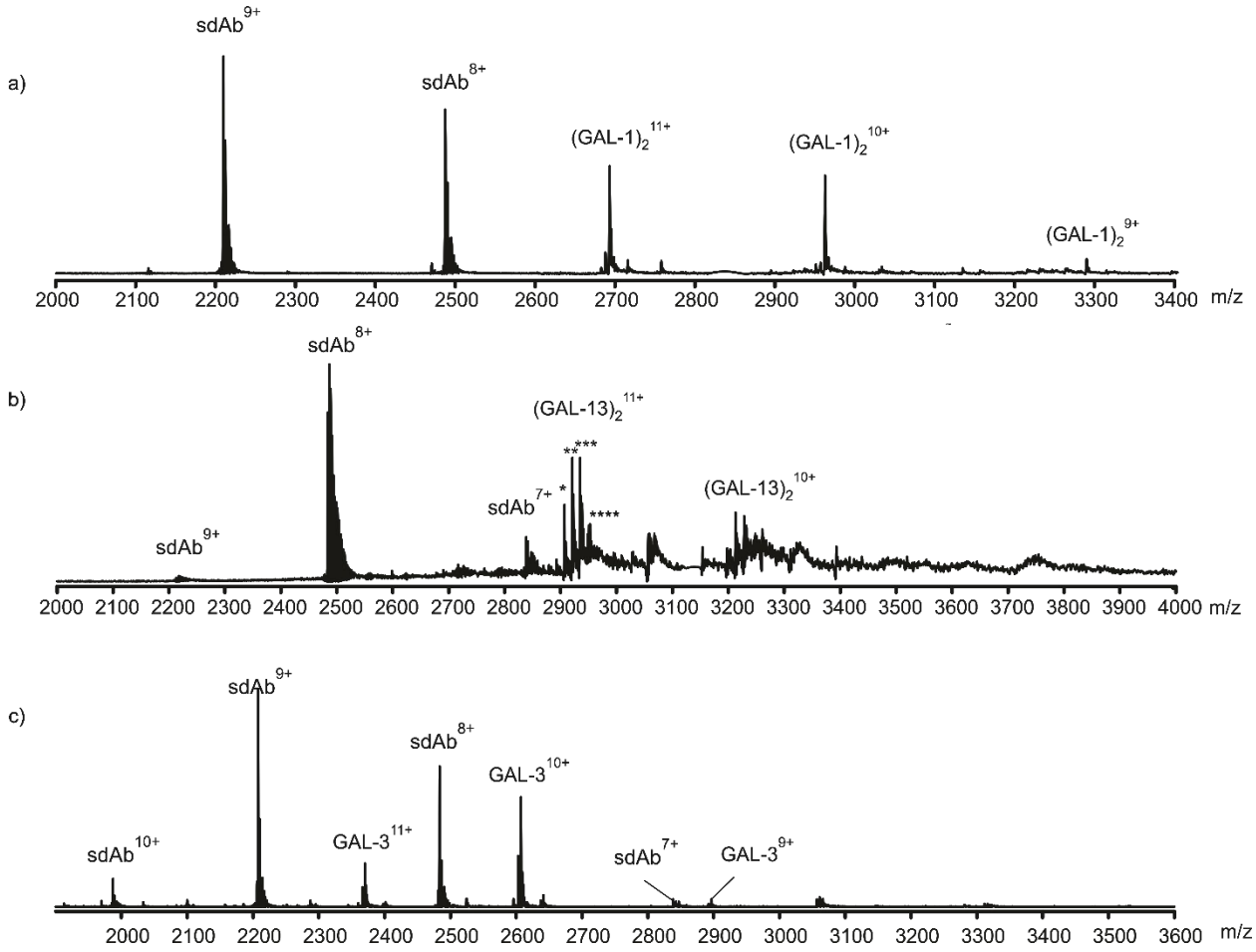

Figure S9. Representative ESI mass spectra acquired in positive ion mode for 200 mM ammonium acetate solutions (pH 7.4, 25 ºC) of sdAb (3 μM) with (a) GAL-1 (5 μM), (b) GAL-13 (15 μM) and (c) GAL-3 (26 μM). * GAL-13 dimer minus 2 methionine, ** GAL-13 dimer minus methionine, *** GAL-13 dimer, **** unidentified post-translation modification of GAL-13 dimer.

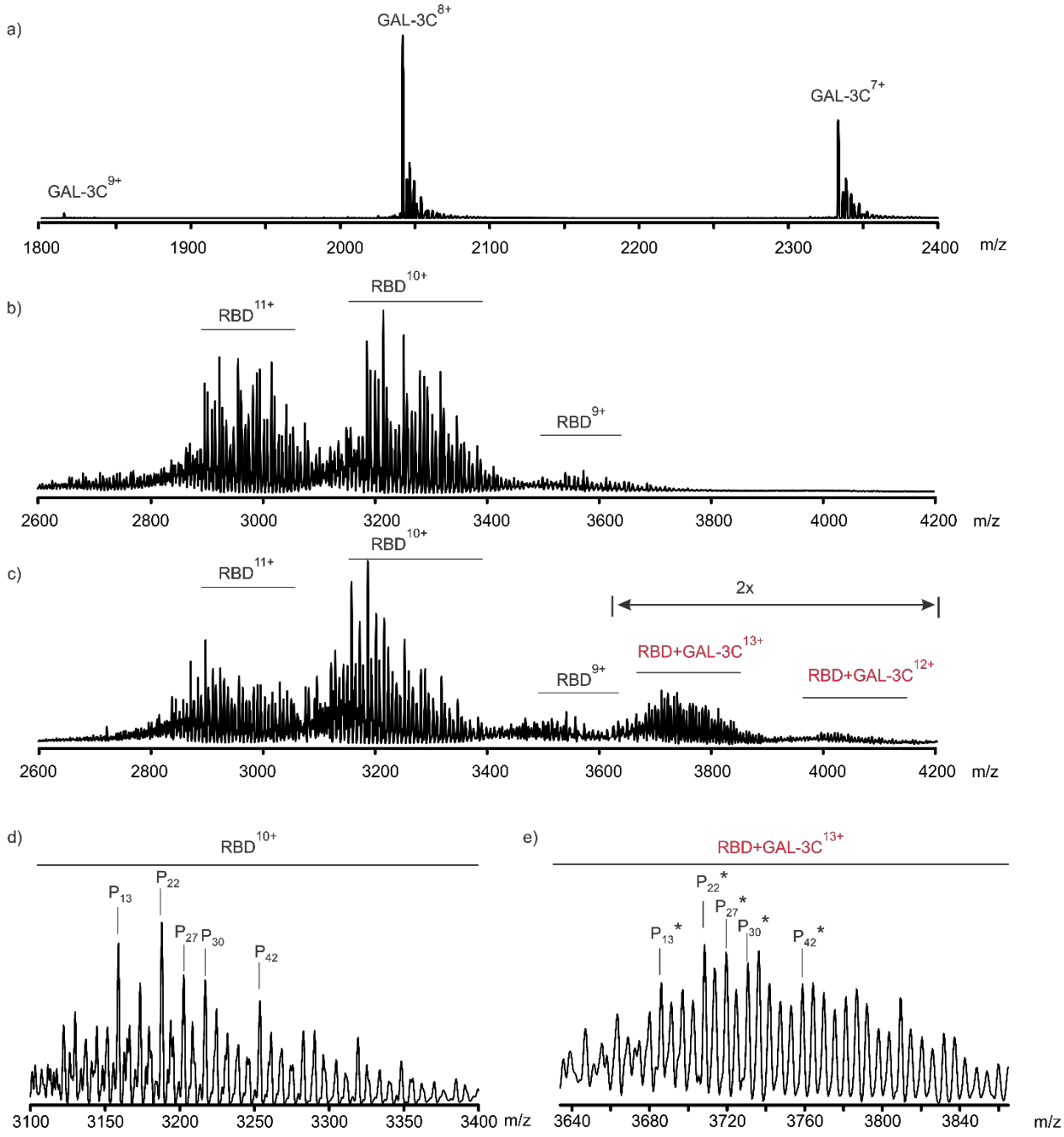

Figure S10. Representative ESI mass spectra acquired in positive ion mode for a 200 mM ammonium acetate solutiond (pH 7.4, 25 ºC) of (a) GAL-3C (5 µM), (b) RBD (5 µM) and (c) RBD (5 µM) and GAL-3C (5 µM). Expanded view of the most abundant charge state of (d) free RBD (10+) and (e) the (RBD+GAL-3C) complex (13+). The most abundant RBD glycoforms are denoted for free RBD (P_i) and the corresponding GAL-3C complex (P_i*).

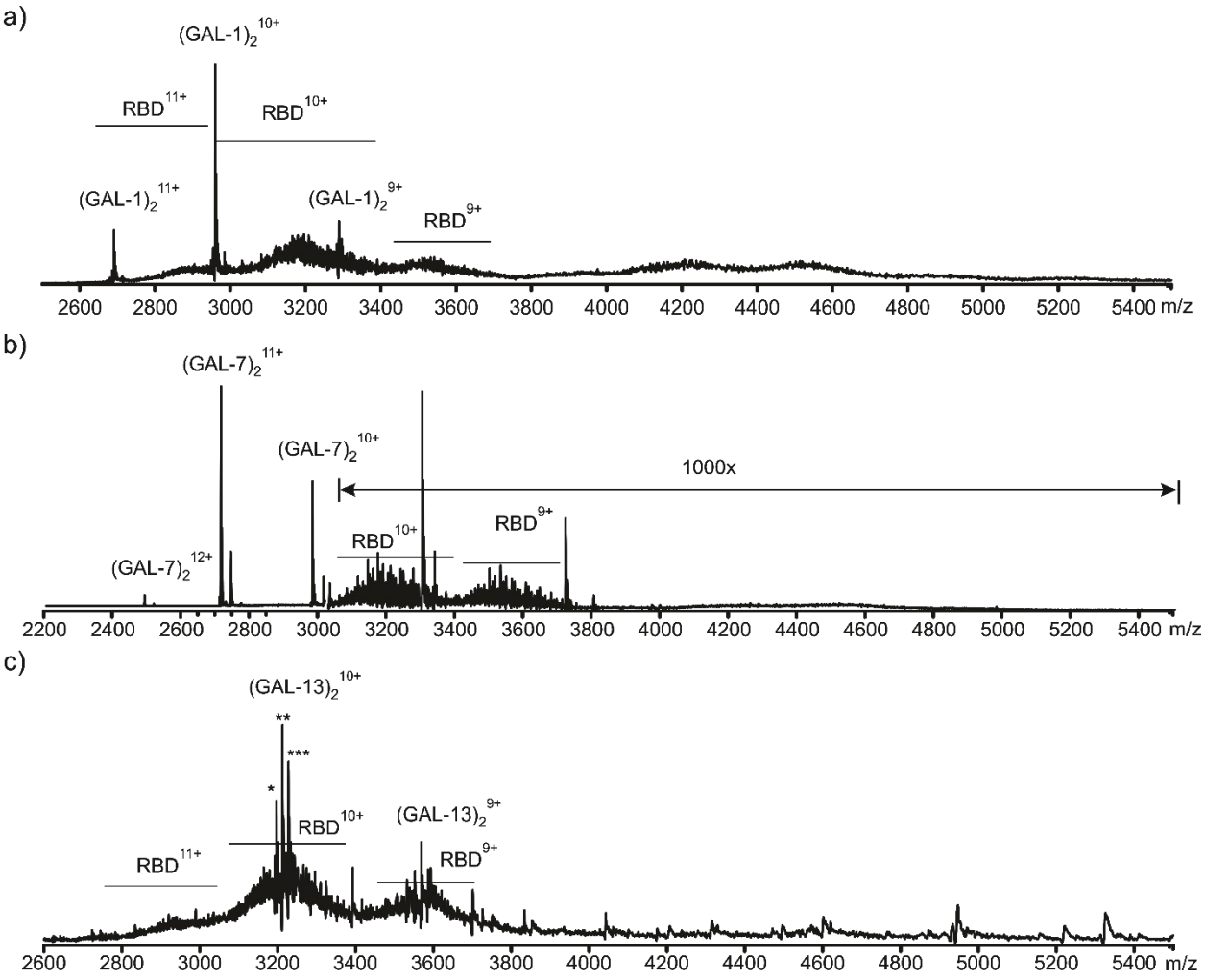

Figure S11. Representative ESI mass spectra acquired in positive ion mode for 200 mM ammonium acetate solutions (pH 7.4, 25 ºC) of (a) GAL-1 (3.5 μM) and RBD (4 μM), (b) Gal-7 (10 μM) and RBD (10 μM) and (c) GAL-13 (3.5 μM) and RBD (4 μM). * GAL-13 dimer minus 2 methionine, ** GAL-13 dimer minus methionine, *** GAL-13 dimer.

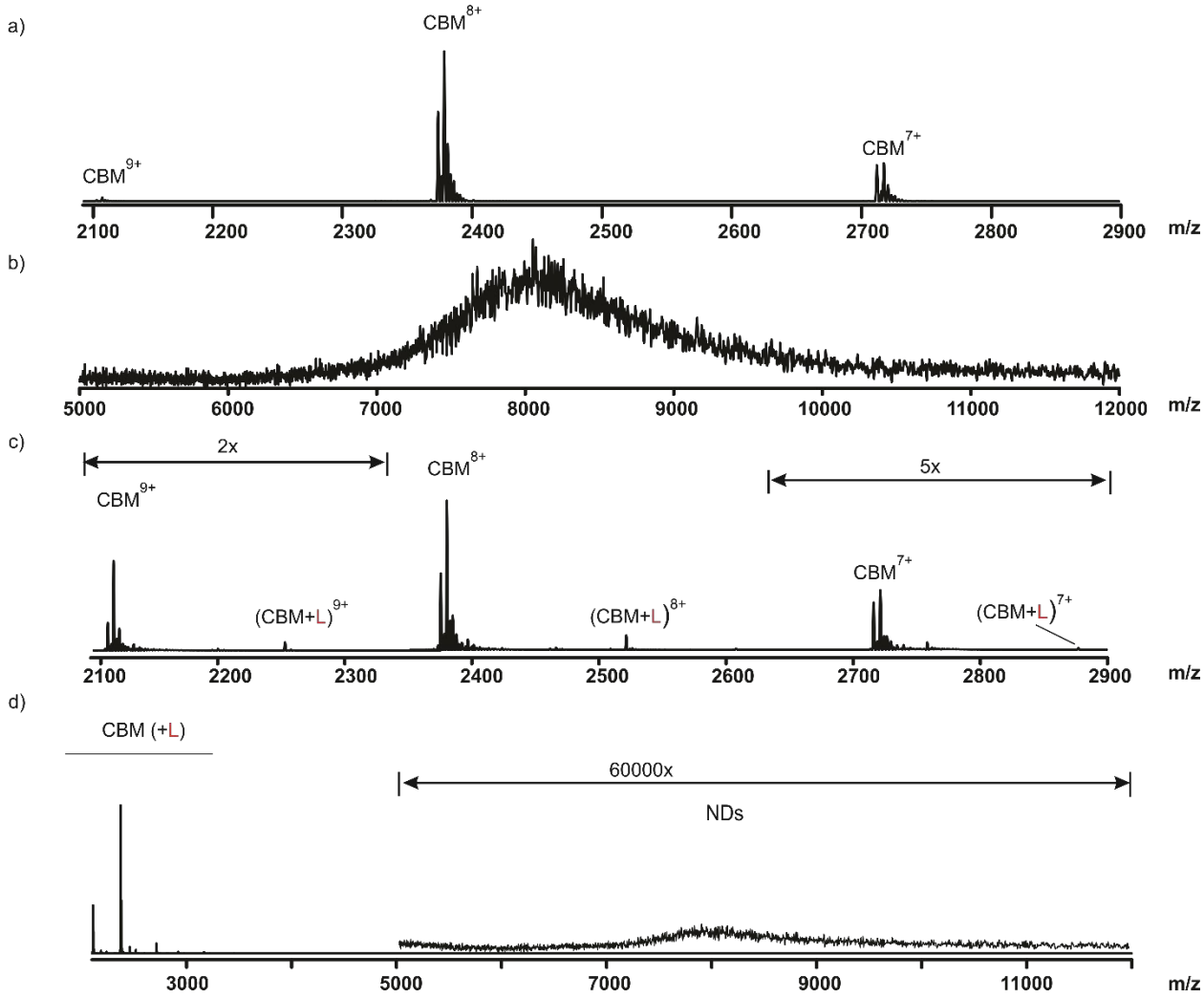

Figure S12. Representative ESI mass spectra acquired in positive ion mode for a 200 mM ammonium acetate solution (pH 6.9, 25 ºC) of (a) CBM (5 μM), (b) ND (4 μM) containing B-tri$_{NGL}$ (L, 120 μM) and (c) CBM (5 μM) and B-tri$_{NGL}$-containing ND (4 μM). (d) Expanded region (m/z 2000-2900) of mass spectrum shown in (c).

References

S1 Vladoiu, M. C.; Labrie, M.; Létourneau, M.; Egesborg, P.; Gagné, D.; Billard, É.; Grosset, A.-A.; Doucet, N.; Chatenet, D.; St-Pierre, Y. Design of a Peptidic Inhibitor That Targets the Dimer Interface of a Prototypic Galectin. *Oncotarget* **2015**, *6*, 40970-40980.

S2 Stowell, S. R.; Arthur, C. M.; Dias-Baruffi, M.; Rodrigues, L. C.; Gourdine, J.-P.; Heimburg-Molinaro, J.; Ju, T.; Molinaro, R. J.; Rivera-Marrero, C.; Xia, B.; Smith, D. F.; Cummings, R. D. Innate Immune Lectins Kill Bacteria Expressing Blood Group Antigen. *Nat. Med.* **2010**, *16*, 295–301.